Article

Kinetics of Redox Polymer-Mediated Enzyme Electrodes

Joshua W. Gallaway, and Scott A. Calabrese Barton

J. Am. Chem. Soc., **2008**, 130 (26), 8527-8536 • DOI: 10.1021/ja0781543 • Publication Date (Web): 07 June 2008

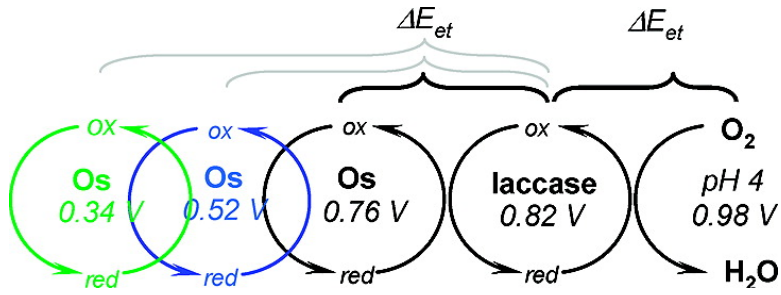

More About This Article

Additional resources and features associated with this article are available within the HTML version:

- Supporting Information
- Links to the 2 articles that cite this article, as of the time of this article download
- Access to high resolution figures
- Links to articles and content related to this article
- Copyright permission to reproduce figures and/or text from this article

View the Full Text HTML

J|A|C|S
ARTICLES

Published on Web 06/07/2008

Kinetics of Redox Polymer-Mediated Enzyme Electrodes

Joshua W. Gallaway[†] and Scott A. Calabrese Barton*[,‡]

Department of Chemical Engineering, Columbia University, New York, New York 10027, and Department of Chemical Engineering and Material Science, Michigan State University, East Lansing, Michigan 48824

Received October 24, 2007; E-mail: scb@msu.edu

Abstract: Oxygen-reducing enzyme electrodes are prepared from laccase of *Trametes versicolor* and a series of osmium-based redox polymer mediators covering a range of redox potentials from 0.11 to 0.85 V. Experimentally obtained current density generated by the film electrodes is analyzed using a one-dimensional numerical model to obtain kinetic parameters. The bimolecular rate constant for mediation is found to vary with mediator redox potential from 250 s^{-1} M^{-1} when mediator and enzyme are close in redox potential to 9.4×10^4 s^{-1} M^{-1} when the redox potential difference is large. The value of the bimolecular rate constant for the simultaneously occurring laccase−oxygen reaction is found to be 2.4×10^5 s^{-1} M^{-1}. The relationship between mediator−enzyme overpotential and bimolecular rate constant is used to determine the optimum mediator redox potential for maximum power output of a hypothetical biofuel cell with a planar cathode and a reversible hydrogen anode. For laccase of *T. versicolor* ($E_e^0 = 0.82$), the optimum mediator potential is 0.66 V (SHE), and a molecular structure is presented to achieve this result.

Introduction

Enzymatic biofuel cells utilize enzyme electrocatalysts to convert chemical energy directly to electrical energy. These devices have the potential to provide a flexible, compact, and inexpensive micropower source, either for devices operating on ambient fuels at mild conditions or for implantable power.[1] The use of purified, concentrated enzymes distinguishes these devices from conventional fuel cells that use noble metal catalysts, or microbial biofuel cells using microorganisms.

In many recently reported biocatalyzed fuel cell systems, including cells based on fructose dehydrogenase and laccase,[2] glucose oxidase−laccase,[3] and glucose oxidase−bilirubin oxidase,[4] oxygen reduction at the biocathode limits the overall rate. These cathodes are limited by mass transfer of oxygen dissolved in solution—required to maintain hydration of the enzyme catalyst—and large electrode thicknesses—required to obtain desired catalyst loading. Each of these requirements is directly tied to issues of catalyst activity, motivating a detailed kinetic study of the oxygen-reducing enzymatic cathode.

A common feature of enzymatic biofuel cells, biosensors, and bioreactors is an enzyme-containing phase that is in electrical contact with an electronically conducting current collector. Electron transport between enzyme catalytic centers and the current collector can be accomplished in two ways. The first is by direct electron transfer (DET), in which enzymes' centers are positioned within electron tunneling distance of the current collector surface. The second is by mediated electron transfer (MET), in which a separate, redox-active mediator species shuttles electrons between enzyme center and the electrode, and optionally acts as an enzyme co-substrate.[5,6] Electrode design requirements for biofuel cells are distinct from those of sensors and bioreactors in that the overall device must be energy-producing. An ideal biofuel cell generates maximum power by simultaneously operating at high current and high cell potential.

To date, the highest reported kinetically limited current densities have been achieved using MET, largely because the mediator allows activation of more than one monolayer of catalyst.[7,8] One approach to MET is to incorporate an enzyme within a cross-linked redox polymer hydrogel, producing a catalytic film that is permeable to ions, electrons, and reactants.[9−11] Redox polymer hydrogels consist of redox-active pendant moieties attached to a water-soluble polymer backbone; in the present case, these moieties are osmium redox complexes. The polymer backbone, concentration of redox species, and redox potential may be varied to control electron transport and reaction kinetics.

Electron transport via these materials may be characterized by an apparent diffusivity, D_{app}. An expression developed by Blauch and Savéant relates D_{app} to redox species concentration in bounded-diffusion systems:[12]

[†] Columbia University.
[‡] Michigan State University.

(1) Calabrese Barton, S.; Gallaway, J.; Atanassov, P. *Chem. Rev.* **2004**, *104*, 4867–4886.
(2) Kamitaka, Y.; Tsujimura, S.; Setoyama, N.; Kajino, T.; Kano, K. *Phys. Chem. Chem. Phys.* **2007**, *9*, 1793–1801.
(3) Barriere, F.; Kavanagh, P.; Leech, D. *Electrochim. Acta* **2006**, *51*, 5187–5192.
(4) Mano, N.; Mao, F.; Heller, A. *ChemBioChem* **2004**, *5*, 1703–1705.
(5) Degani, Y.; Heller, A. *J. Am. Chem. Soc.* **1989**, *111*, 2357–2358.
(6) Palmore, G. T. R.; Kim, H.-H. *J. Electroanal. Chem.* **1999**, *464*, 110–117.
(7) Mano, N.; Fernandez, J. L.; Kim, Y.; Shin, W.; Bard, A. J.; Heller, A. *J. Am. Chem. Soc.* **2003**, *125*, 15290–15291.
(8) Gallaway, J.; Wheeldon, I.; Rincon, R.; Atanassov, P.; Banta, S.; Barton, S. C. *Biosens. Bioelectron.* **2008**, *23*, 1229–1235.
(9) Calabrese Barton, S.; Kim, H. H.; Binyamin, G.; Zhang, Y. C.; Heller, A. *J. Phys. Chem. B* **2001**, *105*, 11917–11921.
(10) Mano, N.; Soukharev, V.; Heller, A. *J. Phys. Chem. B* **2006**, *110*, 11180–11187.
(11) Sun, Y. H.; Calabrese Barton, S. *J. Electroanal. Chem.* **2006**, *590*, 57–65.

$$D_{app} = \frac{1}{6} k_{ex} (\delta^2 + 3\lambda^2) c_m \quad (1)$$

where k_{ex} is the self-exchange rate constant, δ is the electron tunneling distance, λ is the range of bounded motion for the redox sites, and c_m is the redox site concentration. Diffusivity is expected to scale linearly with osmium concentration as the mean distance between centers is reduced.

Selection of optimal mediator architecture for a biofuel cell electrode involves a tradeoff between catalytic rate and cell potential. Generally, the redox potential of the mediator, E_m^0, will determine the operating potential of a mediated biocatalytic electrode.[1] At a cathode, raising the mediator potential to the highest possible value will maximize cell potential. However, this approach may lead to low catalytic rates, which are controlled by the enzyme−mediator overpotential, $\Delta E_{et} = E_e^0 - E_m^0$, where E_e^0 is the redox potential of the enzyme active site. Quantitative optimization of E_m^0 is therefore crucial, as changes in mediator potential of 50 mV or less can cause noticeable variation in catalytic rate.

Previous studies have documented the effect of mediator redox potential on the rate of mediator−enzyme electron transfer.[13−15] Typically, this rate is observed to vary exponentially with reaction free energy, $\Delta G^0 \approx -nF\Delta E_{et}$, a relation generally described by Marcus theory.[16] For unidirectional and rate-limiting electron transfer between enzyme and mediator, the relevant bimolecular rate constant, k_{cat}/K_m, is given by

$$\frac{k_{cat}}{K_m} = Z \exp\left[-\frac{\lambda(1 + \Delta G^0/\lambda)^2}{4RT}\right] \quad (2)$$

where λ is the free energy of molecular reorganization, Z is a frequency factor, R is the gas constant, and T is absolute temperature.[17] Due to the quadratic argument of the exponent, eq 2 predicts a maximum rate at some value of ΔE_{et}, beyond which the rate constant decreases with increasing ΔE_{et}. However, no such "inverted region" is typically observed in enzymatic systems, possibly because the reaction becomes limited by mass transfer or intramolecular electron transfer at high ΔE_{et}.[13,16] For small ΔE_{et}, $-\Delta G^0/\lambda \ll 1$, and eq 2 reduces to a Tafel-like expression,

$$\frac{k_{cat}}{K_m} = \left(\frac{k_{cat}}{K_m}\right)^0 \exp\left[\frac{\alpha F}{RT}\Delta E_{et}\right] \quad (3)$$

where the prefactor $(k_{cat}/K_m)^0$ can be described as a "standard" bimolecular rate constant and α is a symmetry parameter that takes a value of $^1/_2$ for a reversible reaction.

In the case of the laccase biocathode mediated by redox polymers, electrons are transferred from osmium to the T1 copper site of laccase, thus enabling the enzyme to become fully reduced and thereby catalyze the four-electron reduction of dioxygen to water.[18] Kulys and Čenas report results for several enzymes mediated by organic (quinones) and inorganic (ferrocyanide) mediators, and observe the expected free energy relationship followed by a maximal rate at large values of ΔE_{et}.[14,19] However, they do not observe this relationship for laccase (source unspecified), which shows no dependence on mediator potential. Xu considered the reaction of recombinant laccases with several classes of organic mediators (phenols, benzenethiols, anilines, and other aryl compounds), reporting Michaelis−Menten parameters and finding that steric effects from large mediators are fairly minor.[20] Though the expected free energy dependence on ΔE_{et} was observed, no maximum electron transfer rate was apparent, with bimolecular rate constants exceeding 10^8 M^{-1} s^{-1}.

All of these studies focus on solution-phase reactions carried out at conditions of low mediator and high substrate concentrations, and they report optimal transfer rates spanning 3−4 orders of magnitude at large values of ΔE_{et}. Findings from studies of different laccases disagree, in one case showing no potential dependence and in another having no apparent maximum rate. Moreover, it may reasonably be expected that electron transfer may differ significantly in a dense, cross-linked film, where concentrations and ionic strength are high and the enzyme and mediator are entrapped in a hydrogel network, reducing the range of motion for both species.[21]

In this work, we extract the standard bimolecular rate constant, k_{cat}/K_M, obtained at the maximum current density of a laccase biocathode using a range of redox polymer mediators. We then use these rate data to determine the mediator potential at which the maximum power is attained in a hypothetical biofuel cell. Osmium redox polymers were synthesized with redox potentials ranging from 0 V to nearly the redox potential of the laccase itself, approximately 0.82 V (SHE). These were designed using Lever's empirical ligand parameters, which relate the electron-withdrawing nature of ligands to the resulting potential of the central metal atom they bind in transition metal complexes (see Supporting Information).[22] Particular attention is paid to the range of ΔE_{et} from 0 to 400 mV, where the maximum mediated rate constant is expected. This work represents a new method for obtaining enzyme kinetic data in relevant electrochemical systems where multiple physical processes may simultaneously limit electrode performance.

Experimental Section

Materials. Ultrapure O_2, air, N_2, and argon were purchased from Tech Air (White Plains, NY). Laccase from *Trametes versicolor* was purchased from Sigma-Aldrich and purified as previously reported.[23] Vinylimidazole, polyvinylpyridine (PVP, MW = 60 kDa, T_g = 137 °C), ammonium hexachloroosmiate, potassium hexachloroosmiate, 2,2′-bipyridyl (bpy), 4,4′-dimethyl-2,2′-bipyridine (dm-bpy), 4,4′-dimethoxy-2,2′-bipyridine (dmo-bpy), 2,2′:6′,2″-terpyridine (tpy), sodium dithionite, sodium hypophosphite, citric acid monohydrate, sodium citrate, 2-bromoethylamine hydrobromide, acetone, methanol, ethanol, ethylene glycol, dimethylformamide (DMF), and ether were purchased from Fisher Chemical (Fair Lawn, NJ) and used without purification. Azobisisobutyronitrile (AIBN) was purchased from Fisher Chemical and

(12) Blauch, D. N.; Saveant, J. M. *J. Am. Chem. Soc.* **1992**, *114*, 3323–3332.
(13) Zakeeruddin, S. M.; Fraser, D. M.; Nazeeruddin, M. K.; Gratzel, M. *J. Electroanal. Chem.* **1992**, *337*, 253–283.
(14) Kulys, J.; Buchrasmussen, T.; Bechgaard, K.; Razumas, V.; Kazlauskaite, J.; Marcinkeviciene, J.; Christensen, J. B.; Hansen, H. E. *J. Mol. Catal.* **1994**, *91*, 407–420.
(15) Takagi, K.; Kano, K.; Ikeda, T. *J. Electroanal. Chem.* **1998**, *445*, 211–219.
(16) Marcus, R. A.; Sutin, N. *Biochim. Biophys. Acta* **1985**, *811*, 265–322.
(17) Calvo, E. J. In *Encyclopedia of Electrochemistry*; Bard, A. J., Stratmann, M., Eds.; Wiley-VCH: Weinheim, 2003; Vol. 2.
(18) Solomon, E. I.; Sundaram, U. M.; Machonkin, T. E. *Chem. Rev.* **1996**, *96*, 2563–2605.
(19) Kulys, J. J.; Čenas, N. K. *J. Mol. Catal.* **1988**, *47*, 335–341.
(20) Xu, F. *Biochemistry* **1996**, *35*, 7608–7614.
(21) Heller, A. *J. Phys. Chem.* **1992**, *96*, 3579–3587.
(22) Lever, A. B. P. *Inorg. Chem.* **1990**, *29*, 1271–1285.
(23) Hudak, N. S.; Calabrese Barton, S. *J. Electrochem. Soc.* **2005**, *152*, A876–A881.

Chart 1. General Structure of the Synthesized Redox Polymers[a]

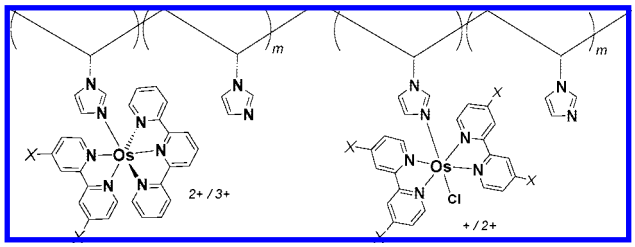

[a] Counterions not shown. In the text, the two forms are signified by the charge of their reduced form. Polymer **2a**, X = Cl; **1b** and **2b**, X = H; **1c** and **2c**, X = CH_3; **1d** and **2d**, X = OCH_3. Polymer **1a**, X = H with the backbone polymer polyvinyl pyridine (not shown).

recrystallized from methanol prior to use. The reagents 4,4′-dichloro-2,2′-bipyridine (dc-bpy, CMS Chemicals Ltd., Oxfordshire, UK) and poly(ethylene glycol) diglycidyl ether (PEDGE, Polysciences Inc., Warrington, PA) were used as received.

Synthesis of Redox Polymers, + Structure. Polyvinylimidazole (PVI) was produced by combining vinylimidazole (20.75 g) and AIBN (0.06545 g) in absolute ethanol for a total volume of 40 mL. The solution was held without stirring at 65 °C for 2 h, to reach an intended conversion of 13.2%.[24] The PVI product was isolated by repeated precipitation in acetone, followed by filtration. The viscosity-average molecular weight, M_v, was found to be 43 kDa by dilute solution viscometry, and the glass transition temperature, T_g, was found to be 177 °C by differential scanning calorimetry.

The osmium complex $[Os(dm\text{-}bpy)_2Cl_2]$ was synthesized in the following way, using methods similar to those reported by Buckingham et al.[25] K_2OsCl_6 (500 mg, 1.04 mmol) was suspended in 40 mL of DMF. Dimethylbipyridine (405 mg, 2.20 mmol) was added, and the mixture was heated to reflux under argon, with stirring, for 45 min. After cooling, the solution was filtered, combined with 20 mL of ethanol, and precipitated in rapidly stirred diethyl ether. The dark red product was filtered and dried in a vacuum overnight. The $[Os(dm\text{-}bpy)_2Cl_2]Cl$ (634 mg) was dissolved in 19 mL of a 2:1 DMF/methanol solution, and 130 mL of an aqueous 1% sodium dithionite solution was added slowly with stirring. After cooling in an ice bath, the crystallized non-electrolyte $[Os(dm\text{-}bpy)_2Cl_2]$ was collected by filtration and dried. Yield: 506 mg, 77%. All other osmium complexes of the form $[Os(x\text{-}bpy)_2Cl_2]$ were synthesized in an analogous fashion.

The osmium complex $[Os(dm\text{-}bpy)_2Cl_2]$ (150 mg, 0.24 mmol) was suspended in 95 mL of ethanol with PVI (210 mg, 2.2 mmol of imidazole) and refluxed with stirring for 3 days.[26] The resulting solution was filtered over a Millipore YM-10 ultrafiltration membrane and dried. Yield: 198 mg. The product (polymer **1c**) was stored as a 10 mg/mL solution in water. All other polymers of the + form (Chart 1) were prepared in an analogous manner and are signified by a **1** followed by a letter, in descending order of redox potential. In the case of polymer **1a**, PVP was substituted for PVI.[27] In order to make the products fully water-soluble, polymers **1a** and **1d** were partially quaternized with an ethylamine group by reacting 2-bromoethylamine hydrobromide with one-fifth of the repeat units. This quaternization is abbreviated as "EA" in the molecular formulas of Table 1 (below).[28]

The osmium loading, *m*, of all redox polymers was determined via inductively coupled plasma mass spectrometry (ICP-MS) conducted by West Coast Analytical Service, Inc. (Santa Fe Springs, CA).

Synthesis of Redox Polymers, 2+ Structure. The osmium complex $[Os(tpy)(dm\text{-}bpy)Cl]Cl_2$ was synthesized as follows. $(NH_4)_2OsCl_6$ (400 mg, 0.91 mmol) was suspended in 10 mL of ethylene glycol. Terpyridine (200 mg, 0.86 mmol) was added, and the mixture was heated to reflux under argon, with stirring, for 15 min. Upon cooling, 10 mL of ethanol was added, and the solution was precipitated in rapidly stirred ether. The blackish-brown product was filtered and dried in a vacuum overnight. This product was assumed to be $[Os(tpy)Cl_3]$ (443 mg, 0.84 mmol), which was combined with 10 mL of ethylene glycol and excess dimethylbipyridine (162 mg, 0.88 mmol) and heated to reflux under argon, with stirring, for 1 h. After cooling, 10 mL of ethanol was added, and the solution was precipitated in ether. The blackish-brown product was collected by filtration and dried. Yield: 342 mg, 53%. All other osmium complexes of the form $[Os(tpy)(x\text{-}bpy)Cl]Cl_2$ were synthesized in an analogous fashion.

PVI was prepared as in the previous section. The complex $[Os(tpy)(dm\text{-}bpy)Cl]Cl_2$ (100 mg, 0.14 mmol) was dissolved in a mixture of 40 mL of deionized water and 5 mL of ethanol. PVI (66 mg, 0.7 mmol of imidazole) was added with stirring. Dropwise, 1 mL of a 10% solution of sodium hypophosphite was added, and the solution was refluxed for at least 13 days, until no further reaction was observed, as monitored by cyclic voltammetry of a test sample. The product was purified by ultrafiltration as in the previous section and dried. Yield: 94 mg. The product (polymer **2c**) was stored as a 10 mg/mL solution in water. All other polymers of the 2+ form (Chart 1) were prepared in the same way.

Laccase Electrode Preparation. The purified laccase enzyme was standardized by spectrophotometric assay with 2,2′-azinobis(3-ethylbenzthiazoline-6-sulfonic acid (ABTS) in 50 mM citrate buffer (pH 4, 40 °C), resulting in an activity of 220 ± 20 U/mg. Assuming 100% protein and a laccase MW of 65 kDa, this is equivalent to a turnover rate of 240 s^{-1}. The redox potential of laccase from *T. versicolor* has been variously reported as 0.78 and 0.82 V (SHE);[9,29] for the current work, it was measured as ~0.82 V by observing the open-circuit potential of a laccase-modified glassy carbon electrode, and this value is used throughout. Redox polymer−laccase film electrodes were made as previously described.[9] Glassy carbon rotating disk electrodes (RDEs) of 3 mm diameter, produced in-house, were sanded with 1200 grit ultrafine sandpaper (Buehler, IL), and polished with 0.3- and 0.05-μm alumina slurries, followed by sonication for 10 min in deionized water. After the cleaning procedure, no electrochemical features would be visible for the bare electrode between hydrogen and oxygen evolution in pH 4, 100 mM citrate buffer at 50 mV/s scan rate. A solution of the desired redox polymer (10 mg/mL) was combined with laccase solution (20 mg/mL), and PEGDGE cross-linker (5 mg/mL) was added in amounts necessary for a solute composition of 61% polymer, 32% laccase, and 7% cross-linker. This composition was found to be optimum for polymers **1c** and **2c**, and assumed to hold for the remaining polymers. A 5 μL aliquot of this solution was pipetted onto the electrode surface for a material loading of 0.693 mg/cm^2. The electrode cured for 5 h at room temperature in a low-humidity environment, RH < 10%.

Electrochemical Instrumentation. All electrochemical experiments were carried out in a water-jacketed cell containing 100 mL of pH 4, 0.1 M citrate buffer with a jacket temperature of 40 °C. Glassy carbon RDEs were constructed from 3 mm diameter, type 1 glassy carbon rods (Alfa Aesar, Ward Hill, MA). Measurements were performed with a μAutolab III potentiostat (Eco Chemie). Electrodes were rotated using a Pine Instruments rotator. Potentials were measured relative to a silver−silver chloride (3 M NaCl) reference electrode (BAS, West Lafayette, IN). Platinum gauze was used as the counter electrode. Impedance was measured using a Schlumberger SI 1255 frequency response analyzer. Correction of potentials for ohmic resistance, where noted, was performed by

(24) Dambatta, B. B.; Ebdon, J. R. *Eur. Polym. J.* **1986**, *22*, 783–786.
(25) Buckingham, D. A.; Dwyer, F. P.; Goodwin, H. A.; Sargeson, A. M. *Aust. J. Chem.* **1964**, *17*, 325–336.
(26) Forster, R. J.; Vos, J. G. *Macromolecules* **1990**, *23*, 4372–4377.
(27) Aoki, A.; Rajagopalan, R.; Heller, A. *J. Phys. Chem.* **1995**, *99*, 5102–5110.
(28) Bohmer, M. R.; Heesterbeek, W. H. A.; Deratani, A.; Renard, E. *Colloids Surf. A,* **1995**, *99*, 53–64.
(29) Xu, F.; Shin, W. S.; Brown, S. H.; Wahleithner, J. A.; Sundaram, U. M.; Solomon, E. I. *Biochim. Biophys. Acta* **1996**, *1292*, 303–311.

measuring high-frequency resistance, R_Ω, or the real electrochemical impedance of the cell at a modulating frequency of 100 kHz. R_Ω was found to be 179 ± 2 Ω for all samples, including a bare glassy carbon electrode, a value attributable to migration resistance in the bulk electrolyte. The relation $R_\Omega = (4\kappa r_o)^{-1}$, with r_o the disk electrode radius, yields a buffer conductivity $\kappa = 9.4$ mS cm^{-1} at 40 °C, within the expected range.

Concentration and Diffusion Measurements. Osmium concentration in the laccase films was determined by preparing 3 mm diameter enzyme-containing films, identical to those used on the RDEs, on silicon wafers. The formulation described above was deposited and cured, and profiles of the resulting films were scanned using an Alpha-Step IQ surface profiler (KLA-Tencor, San Jose, CA), a force-based profilometry system. Multiple orthogonal scans were used to calculate an average thickness, from which volume and concentration could be determined using the known mass loadings of osmium and enzyme (see Supporting Information). This concentration was assumed to hold for films cast on electrodes. Active osmium concentration, as determined by coulometry, was generally less than but within 40% of these values (see Supporting Information).

Inclusion of metal complexes within bulk PVI hydrogel matrices has been shown to dramatically reduce swelling capacity to no more than a factor of ~1.5 at pH 4.[30,31] We did not detect swelling of the non-quaternized enzyme films by either optical microscopy or profilometry, and therefore concentrations for immersed electrode films are assumed to be the same as in dry conditions (see Supporting Information). A swelling factor of 1.6 was observed for the EA-quaternized polymer **1d**, and a literature value of 2.2× swelling was used for the EA-quaternized PVP-based polymer **1a** (see Supporting Information).[27] The film thicknesses listed in Table 2 (below) account for this swelling.

Apparent electron diffusion of the mediator, D_m, was calculated from the current response following a potential step, using the Cottrell equation:[32]

$$i(t) = \frac{nFc_m D_m^{1/2}}{\pi^{1/2}} t^{-1/2} \quad (4)$$

where i is the observed current density following a potential step, n is the stoichiometric coefficient for electron transfer, F is Faraday's number, and t is time after the step. In quiescent, nitrogen-saturated solution, the working electrode was held at a reducing potential until negligible current was recorded.[33,34] The potential was stepped to an oxidizing potential, and after an initial nonlinear regime, current decayed linearly to zero with the inverse square root of time, indicating an apparent Fickian diffusion of charge.[35] The slope in the 10−30 ms period following the potential step, wherein the response was linear for all samples, was used to calculate D_m. Figure 2 (inset) displays an example time history for polymer **2b**.

Enzyme Electrode Model. In order to determine kinetic parameters for the catalytic reaction in the film, the system was modeled as described in detail elsewhere.[36,37] We assume the enzyme reaction for oxygen substrate (s) and mediator (m) may be characterized by a ping-pong bi-bi scheme, given as[38]

$$S + E_{red} \underset{k_{-1s}}{\overset{k_{1s}}{\rightleftharpoons}} ES \xrightarrow{k_{2s}} P + E_{ox} \quad (5)$$

$$M_{red} + E_{ox} \underset{k_{-1m}}{\overset{k_{1m}}{\rightleftharpoons}} EM \xrightarrow{k_{2m}} M_{ox} + E_{red} \quad (6)$$

Assuming that the concentration of complexes ES and EM remains at steady state, an expression for the homogeneous reaction rate may be obtained from this scheme. Governing equations for the biocathode film follow from steady-state, one-dimensional material balances on the substrate and reduced mediator complex, considering transport only by diffusion:

$$D_m \frac{\partial^2 c_m}{\partial x^2} = \frac{k_{cat} K_m^{-1} c_e c_m c_s}{c_m K_m^{-1}(c_s + K_s) + c_s} \quad (7)$$

$$D_s \frac{\partial^2 c_s}{\partial x^2} = \frac{\frac{1}{4} k_{cat} K_m^{-1} c_e c_m c_s}{c_m K_m^{-1}(c_s + K_s) + c_s} \quad (8)$$

where the right sides of eqs 7 and 8 contain the homogeneous reaction rate as derived from the ping-pong bi-bi scheme, with overall rate constant k_{cat} and apparent Michaelis constants K_m and K_s,[39] defined as[40,41]

$$k_{cat} = \frac{k_{2s}k_{2m}}{(k_{2s} + k_{2m})}; \quad K_m = \frac{k_{2s}(k_{-1m} + k_{2m})}{k_{1m}(k_{2s} + k_{2m})}; \quad K_s = \frac{k_{2m}(k_{-1s} + k_{2s})}{k_{1s}(k_{2s} + k_{2m})} \quad (9)$$

Variables c_e, c_m, and c_s denote the concentrations of enzyme, reduced mediator, and oxygen substrate. Here we assume a stoichiometric coefficient for electrons, $n = 1$.

At the film−electrode boundary, $x = 0$, there is no substrate flux, and the mediator concentration is controlled by the working electrode potential, V, through a Butler−Volmer expression:

$$x = 0: \frac{dc_s}{dx} = 0, \; i = -nFD_m \frac{dc_m}{dx} = i_o \left\{ \left(1 - \frac{c_m}{c_m^o}\right) \exp\left[-\frac{V - E^0}{b}\right] - \frac{c_m}{c_m^o} \exp\left[\frac{V - E^0}{b}\right] \right\} \quad (10)$$

where c_m^o is the known total mediator concentration, in both reduced and oxidized forms, and i_o the exchange current density. The Tafel slope, b, is an adjustable parameter introduced to capture the quasi-reversibility of the redox reaction at the electrode surface (Supporting Information). Values of b obtained by numerical fitting of cyclic voltammograms are listed in Table 2.

At the film−solution boundary, $x = \phi$, where ϕ is the film thickness, there is no flux of mediator out of the film, and the substrate is assumed to be at its bulk concentration, c_s^o:

$$x = \phi: \frac{dc_m}{dx} = 0, \; c_s = c_s^o \quad (11)$$

The latter assumption neglects any film−solution partition coefficient for oxygen and assumes uniform oxygen concentration external to the film. In the context of RDE experiments, this is equivalent to a condition of infinite rotation speed, which we approximate using Koutecky−Levich analysis.[32]

This system of differential equations is easily solved using finite difference methods, to obtain the concentration profiles $c_m(x)$ and

(30) Pekel, N.; Salih, B.; Guven, O. *J. Mol. Catal. B* **2003**, *21*, 273–282.
(31) Ybarra, G.; Moina, C.; Molina, F. V.; Florit, M. I.; Posadas, D. *Electrochim. Acta* **2005**, *50*, 1505–1513.
(32) Bard, A. J., and Faulkner, L. R. *Electrochemical methods: fundamentals and applications*, 2nd ed.; John Wiley: New York, 2001.
(33) Forster, R. J.; Kelly, A. J.; Vos, J. G.; Lyons, M. E. G. *J. Electroanal. Chem.* **1989**, *270*, 365–379.
(34) Forster, R. J.; Vos, J. G. *J. Electroanal. Chem.* **1991**, *314*, 135–152.
(35) Majda, M. In *Molecular Design of Electrode Surfaces*; Murray, R. W., Ed.; Wiley: New York, 1992; Vol. 159, p 206.
(36) Bartlett, P. N.; Pratt, K. F. E. *J. Electroanal. Chem.* **1995**, *397*, 61–78.
(37) Calabrese Barton, S. *Electrochim. Acta* **2005**, *50*, 2145–2153.
(38) Limoges, B.; Moiroux, J.; Saveant, J.-M. *J. Electroanal. Chem.* **2002**, *521*, 1–7.
(39) Ogino, Y.; Takagi, K.; Kano, K.; Ikeda, T. *J. Electroanal. Chem.* **1995**, *396*, 517–524.
(40) Cleland, W. W. *Biochim. Biophys. Acta* **1963**, *67*, 104–137.
(41) Kano, K.; Ikeda, T. *Anal. Sci.* **2000**, *16*, 1013–1021.

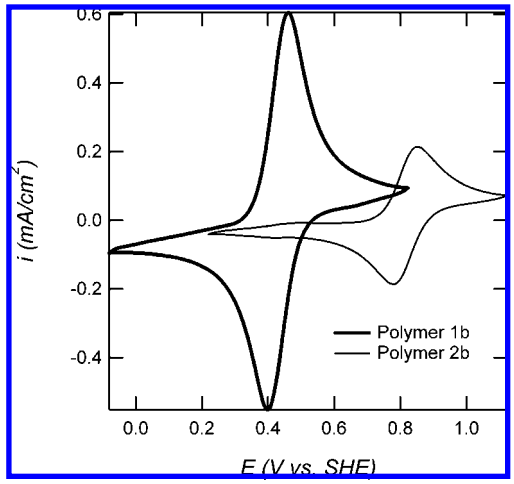

Figure 1. Cyclic voltammograms of representative enzyme electrode films of polymers **1b** and **2b**, showing the osmium redox couple. Experiments are in quiescent N_2-saturated 100 mM citrate buffer, pH 4, at 40 °C. Scan rates are 50 mV/s.

Table 1. Series of Redox Polymers

polymer	formula	E^0/V (SHE)	Os (wt %)	ref
2a	poly(*n*-VI_{30}[Os(tpy)(dc-bpy)]$^{2+/3+}$)	0.85	5.5	
2b	poly(*n*-VI_{15}[Os(tpy)(bpy)]$^{2+/3+}$)	0.82	9.2	42
2c	poly(*n*-VI_{23}[Os(tpy)(dm-bpy)]$^{2+/3+}$)	0.77	6.6	9
2d	poly(*n*-VI_{28}[Os(tpy)(dmo-bpy)]$^{2+/3+}$)	0.69	5.6	
1a	poly((VP_{12}[Os(bpy)$_2$Cl]$^{+/2+}$)(VP_5-EA))	0.52	9.1	27
1b	poly(*n*-VI_{12}[Os(bpy)$_2$Cl]$^{+/2+}$)	0.43	11	26
1c	poly(*n*-VI_{24}[Os(dm-bpy)$_2$Cl]$^{+/2+}$)	0.40	6.5	43
1d	poly((*n*-VI_{55}[Os(dmo-bpy)$_2$Cl]$^{+/2+}$) (n-VI_5-EA))	0.11	2.6	44

$c_s(x)$. The current density may then be calculated by eq 10, and compared to experimental results corrected by Koutecky−Levich analysis.

Results

Mediator Redox Potential and Loading. Eight water-soluble redox polymers were produced, each by the reaction of an osmium metal complex with a water-soluble polymer. By changing the Lewis base character of the ligands bonded to the central osmium atom, the polymers were designed to manifest a range of redox potentials, beginning near the potential of laccase from *T. versicolor* and extending to more reducing potentials. Cyclic voltammograms for enzyme electrodes of polymer **1b** and **2b** in the absence of oxygen are show in Figure 1. In every case, the produced polymer expressed a single redox couple, as measured by cyclic voltammetry, and the redox potential E^0_m was within about 50 mV of the value predicted from a Lever analysis (Supporting Information).[22] Formulas for these polymers are shown in Table 1, along with experimentally determined physical parameters and previous literature citations. Osmium loading varied substantially among these materials, even though each charge group (+ and 2+) was prepared with a consistent procedure.

Biocatalytic electrode films produced from each of the polymers differ in several respects—density ρ, film thickness ϕ, osmium concentration c_m, enzyme concentration c_e, apparent electron diffusivity D_m, and regeneration kinetics at the film−electrode interface. The latter was observed primarily as variable peak separation in cyclic voltammetry, and was empirically accounted for by adjustment of the Tafel slope, b, in eq 10. Measured values of these parameters for each polymer are presented in Table 2.

We note that the current peak heights displayed in Figure 1 fall below that predicted assuming semi-infinite diffusion, using the Randles−Sevçik equation and the parameters of Table 2. In fact, bounded diffusion was detected at scan rates of 50 mV s^{-1} and below by demonstrating that current peak height varied linearly with scan rate (Supporting Information). For this reason, cyclic voltammograms of the type shown in Figure 1 were only used to estimate mediator redox potential, E^0, and Tafel slope, b (see Supporting Information).

Figure 2 shows the observed relationship between D_m and c_m for all polymers, as obtained by Cottrell analysis. The expected linear relationship is observed for most polymers, within experimental error. Electron transport properties are therefore shown to be independent of redox potential or the general molecular structure of the polymer and directly related to the concentration of osmium centers. Deviations in this linear relationship can be explained by variations in molecular mobility, characterized by the parameter λ in eq 1. For example, the deviation from linearity observed for polymer **2d** may be explained by the substitution of polar methoxy groups in polymer **2d** as compared to the nonpolar methyl groups in **2c**.

Catalytic Performance of Films. Representative polarization curves for oxygen reduction in oxygen-saturated buffer catalyzed by laccase electrodes mediated by polymers **1b** and **2b** are shown in Figure 3a. As the working electrode potential falls below the redox potential of the mediator, catalytic current initiates, increasing with decreasing potential until a current plateau i_{pl} is reached. The plateau current value depends on several phenomena: substrate and electron transport; concentrations of mediator, enzyme, and substrate; enzyme kinetics of the catalytic reaction; and film thickness.[32,36,45] When values of i_{pl} for all eight enzyme electrodes are examined, a weak correlation with mediator redox potential is observed, as shown in Figure 3b. The highest-potential polymers, **2a** and **2b**, generate low current density, despite having average osmium concentration and charge transport values (Figure 2). This is attributed to a low overpotential, ΔE_{et}, between the mediator and the laccase enzyme, indicative of a low thermodynamic driving force for electron transfer. As this overpotential between enzyme and mediator increases, less correlation between mediator potential and i_{pl} is observed, **2c** and **1c** being similar despite a 375 mV difference in their redox potentials, **1a** and **1b** being quite high, and **1d** being low despite having the largest ΔE_{et} value with respect to the laccase enzyme.

The highest current density reported to date for an oxygen-reducing biocathode film on a planar electrode of the type presented here is 1.2 mA/cm^2, for a biocathode prepared from laccase of *Coriolus hirsutus* and a redox polymer similar in structure to polymer **2c**, operating at 37 °C and 1600 rpm with 1 atm saturated oxygen in 0.2 M citrate buffer, pH 5.[9] In the

(42) Gao, Z. Q.; Binyamin, G.; Kim, H. H.; Barton, S. C.; Zhang, Y. C.; Heller, A. *Angew. Chem., Int. Ed.* **2002**, *41*, 810–813.
(43) Ohara, T. J.; Rajagopalan, R.; Heller, A. *Anal. Chem.* **1994**, *66*, 2451–2457.
(44) Taylor, C.; Kenausis, G.; Katakis, I.; Heller, A. *J. Electroanal. Chem.* **1995**, *396*, 511–515.
(45) Andrieux, C. P.; Dumas-Bouchiat, J. M.; Saveant, J. M. *J. Electroanal. Chem.* **1982**, *131*, 1–35.

Table 2. Physical Parameters of Redox Polymer−Laccase Films

polymer	density (g/cm^3)	film thickness (ϕ, μm)	c_m (mM)	c_e (mM)	$D_m \times 10^9$ (cm^2/s)	Tafel slope (b, mV)
2a	1.2 ± 0.054	0.29 ± 0.05	220 ± 10	6.1 ± 0.27	0.99 ± 0.22	45 ± 6
2b	1.1 ± 0.12	0.89 ± 0.25	300 ± 30	5.1 ± 0.56	1.4 ± 0.16	58 ± 6
2c	1.1 ± 0.058	0.54 ± 0.09	240 ± 10	5.6 ± 0.30	1.2 ± 0.17	59 ± 2
2d	1.2 ± 0.13	1.2 ± 0.05	210 ± 20	5.8 ± 0.63	0.50 ± 0.17	60 ± 4
1a	1.5 ± 0.097	1.0 ± 0.11[a]	430 ± 30	7.4 ± 0.48	2.2 ± 0.54	37 ± 3
1b	1.5 ± 0.092	0.6 ± 0.10	540 ± 35	7.5 ± 0.46	2.3 ± 0.34	55 ± 2
1c	1.3 ± 0.13	1.1 ± 0.11	240 ± 25	5.6 ± 0.56	1.4 ± 0.31	90 ± 3
1d	1.2 ± 0.16	6.0 ± 0.41[a]	100 ± 15	6.0 ± 0.80	0.11 ± 0.010	95 ± 6

[a] Thickness increased due to hydration. See Supporting Information.

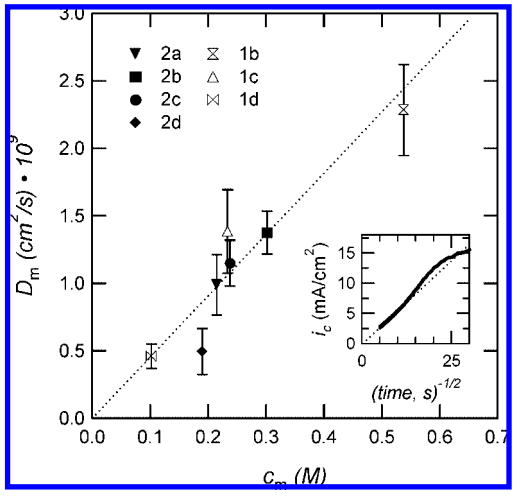

Figure 2. Relationship of film charge transport (D_m) with osmium concentration (c_m) for biocathodes prepared from each of the redox polymer mediators and laccase. All experiments are in quiescent N_2-saturated 100 mM citrate buffer, pH 4, at 40 °C. Error bars represent the standard deviation of five experiments on different electrodes. Best-fit line passing through the origin with a slope of $(4.54 \pm 0.35) \times 10^{-9}$. Inset shows a Cottrell plot for an enzymatic film prepared from polymer **2b**, with slope for the linear region disappearing into the origin.

present work, this is exceeded by polymers **1a** and **1b** by nearly a factor of 2 at 900 rpm, at pH 4 and 40 °C.

Mass transport of dissolved oxygen substrate external to the film was considered using Koutecky−Levich analysis, as shown in Figure 4.[45] The plateau current was measured as a function of rotation rate and plotted as the inverse square root of rate versus the inverse of the plateau current. All biocathodes produced linear Koutecky−Levich plots at all substrate concentrations, allowing extrapolation to the ordinate to determine the mass-transport-corrected plateau current limit, $i_{pl,k}$:

$$\frac{1}{i_{pl}} = \frac{1}{i_l} + \frac{1}{i_{pl,k}}; \quad i_l = m_l \omega^{1/2} \tag{12}$$

where $i_l = m_l\, \omega^{1/2}$ is a current based on the external mass transport limitation, which is dependent on electrode rotation rate, ω. Measured film thickness was generally 1 μm or less, much less than the calculated diffusion layer thickness for these experiments (11 μm at 3600 rpm).

Films produced from high ΔE_{et} polymers (**1a**−**d**) have slopes similar to those shown for polymer **1b**: $m_l = 7.6 \pm 1.6$ rpm$^{1/2}$ cm^2 mA^{-1} under saturated oxygen and $m_l = 35 \pm 2.0$ rpm$^{1/2}$ cm^2 mA^{-1} under 25% oxygen in nitrogen. Under conditions where oxygen concentration is uniform within the film, i_l (ω) follows the Levich equation, and m_l is directly related to the bulk diffusivity of oxygen. Using the values above, and assuming an oxygen-reduction electron transfer coefficient $n = 4$, the oxygen diffusion coefficient in the buffer was found to be 1.5×10^{-5} cm^2/s, half the nominal value of 3×10^{-5}.[32,46] This factor of 2 is likely explained by non-unity partitioning of oxygen into the film.

For the cases of polymers with low ΔE_{et} values (**2a**−**d**), slopes at high oxygen concentration are lower than predicted, 4.6(±0.80) shown for polymer **2b**. This is explained by poor enzyme kinetics at low ΔE_{et}, in which case the enzyme reaction is saturated in oxygen and approaches zero-order dependence on oxygen concentration.

Variation of bulk oxygen concentration from 1 atm O_2 to 1 atm N_2 reveals the kinetic character of the films, as shown for **1b** and **2b** in Figure 5a. Response to a 4-fold increase in oxygen from 0.25 to 1 is nonlinear in both cases, resulting in a 2.6-fold increase in $i_{pl,k}$ for **1b** and a 1.3-fold increase for **2b**, which becomes virtually saturated as described above. These polymers are representative of their charge groups, with the + reduced charge group showing decreased saturation compared to polymers of the 2+ group.

Determination of Kinetic Parameters, Sensitivity to Substrate. The rate of oxygen reduction at the film-modified electrode may be limited by one or more processes, namely enzyme kinetics, charge transport via the mediator, mass transport of oxygen substrate internal or external to the film, and ion transport (primarily external to the film).[45] Prior to fitting to the numerical model, the experimental data were corrected to account for transport limitations external to the film that are not considered in the model. Specifically, external oxygen transport limitations were accounted for by Koutecky−Levich analysis, and *iR* correction was applied to all electrode potentials to account for finite conductivity in the bulk electrolyte. The main remaining limiting processes were enzyme kinetics and charge transport, both of which impact electrode performance under nearly all conditions.

Charge transport was quantified by estimating D_m as summarized in Table 2. This allowed the kinetic parameters k_{cat}, K_m, and K_s (eqs 7 and 8) to be estimated by fitting a numerical solution of the film electrode model to appropriate experimental data. The differential equations were solved using the finite difference method and a nonlinear, coupled differential equation solver.[47] Example data sets used for fitting are given in Figure 5 for polymers **1b** and **2b**.[48]

Numerical predictions of current density comparable to the data in Figure 5 were then obtained for enzyme electrodes made with each polymer. Plateau current density was calculated at a fixed electrode potential, 0 V (SHE), for five different bulk substrate concentrations c_s^o; these results were comparable to experimental data as exemplified by Figure 5a Results were also

(46) Jordan, J.; Ackerman, E.; Berger, R. L. *J. Am. Chem. Soc.* **1956**, *78*, 2979–2983.

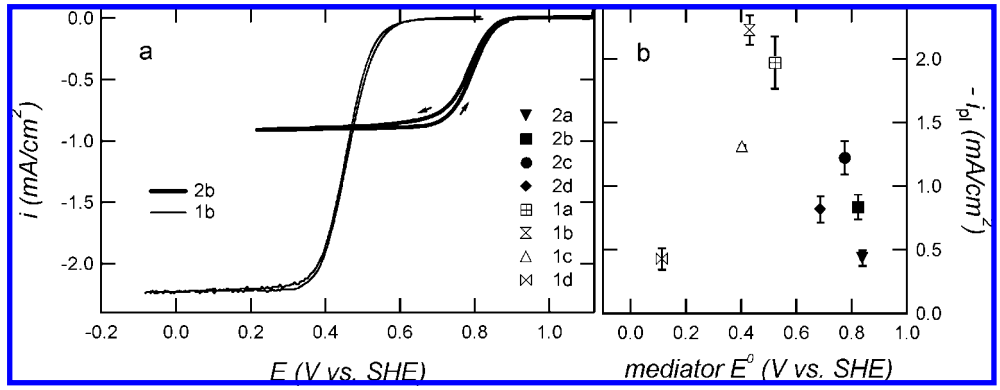

Figure 3. Cathode performance of enzyme electrodes prepared with each redox polymer. (a) Polarizations curves for polymers **2b** and **1b**. (b) Plateau current values for all polymers. Experiments conducted in 1 atm O_2-saturated citrate buffer at 900 rpm rotation, scan rate 1 mV/s initiated at highest potential. All other conditions as in Figure 2. Error bars indicate standard deviation of at least four independent experiments.

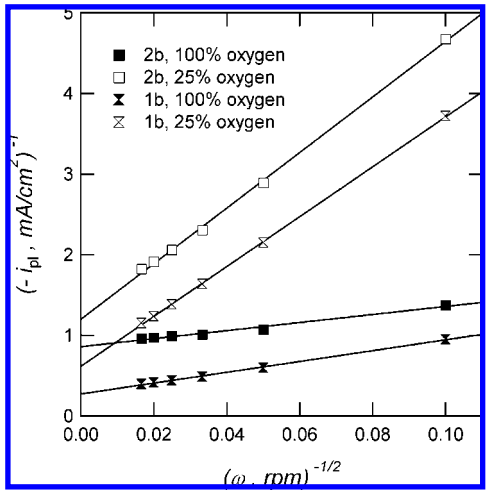

Figure 4. Koutecky−Levich plots showing the dependence of plateau current density on electrode rotation rate, ω. Conditions are as in Figure 3 unless otherwise indicated. Best-fit lines are linearly extrapolated to the ordinate to predict current density for $\omega \rightarrow \infty$.

calculated with c_s^o fixed at 1 atm over a polarization range of 1−0 V (SHE), comparable to data shown in Figure 5b. Potential variations achieved variation in concentration of reduced mediator, the enzyme co-substrate, at the electrode−film interface. Predicted values from the numerical model were fit simultaneously to respective experimental data that were both ohmic and Koutecky−Levich corrected. This approach makes it possible to extract values of k_{cat}, K_s, and K_m from a simultaneous fit in which both substrate and mediator concentrations are varied, the latter by variations in potential. The reaction rate at the mediator−electrode boundary was assumed to be fast ($i_o \rightarrow \infty$).[32] To account for departures from a purely Nernstian process, the Tafel slope, b, was determined from the peak separation of cyclic voltammograms in the absence of oxygen, as shown in Figure 1. Values of b for each polymer are given in Table 2.

Results of the nonlinear least-squares fits are shown in Figure 5a for plateau current values and Figure 5b for polarization in oxygen-saturated buffer. Values for the three kinetic parameters k_{cat}, K_s, and K_m, are given in Table 3. Unique parameters were obtained for polymers **2a**−**d** and **1a**,**b**. Reported error estimates are 1σ confidence intervals calculated from the residuals and covariance of the fitted parameters.

At high values of ΔE_{et}, precise determination of all three kinetic parameters was impossible because the electrode is mediator-saturated ($c_m^o \gg K_m$) and model predictions are insensitive to variation in K_m. Therefore, for **1c** and **1d**, the bimolecular rate constants (k_{cat}/K_m, k_{cat}/K_s) could be obtained from curve fits, but independent values of k_{cat} could not. However, one may reasonably assume that k_{cat} does not vary greatly among the polymers with high ΔE_{et}.

The k_{cat} values found generally agree with spectrophotometric data for laccase from *T. versicolor* dissolved in bulk solution-phase with osmium complexes and oxygen as substrates.[49] The global rate constant k_{cat} as reported in Table 3 is written with respect to mediator turnover. To convert to oxygen turnover rate, this k_{cat} must be divided by 4, resulting in values between 22 and 110 s^{-1}.

The various mediator structures lead to varying oxygen sensitivity in the resulting electrodes, as observed in Figure 5. While oxygen Michaelis constants, K_s, do not vary greatly, enzyme electrodes prepared from high-potential mediators appear to become oxygen-saturated at low oxygen concentrations. This effect is due to mediator saturation. Figure 6 shows simulated profiles for the concentrations of oxygen, c_s, and reduced mediator, c_m, within the film, along with the normalized local catalytic reaction rate. In the case of polymer **2b**, reaction rate is partially controlled by the mediator concentration, decreasing where reduced mediator concentration is low. For polymer **1b**, which is saturated in mediator, reaction rate is affected only by the concentration of oxygen at the film boundary, which is determined by RDE rotation rate. Calculated values of K_s ranged from 400 to 2000 μM. Literature values for laccase−oxygen K_s are variously reported as 20−50, 300−400, and 80−1000 μM for film electrodes of several different natures and structures.[50–53]

(47) Newman, J. *Ind. Eng. Chem. Fund.* **1968**, *7*, 514–517.
(48) An alternative to Koutecky−Levich analysis is to include external mass transport of oxygen explicitly in the film electrode model, by introducing a mass transfer boundary condition at the film−electrolyte interface (eq 8). Though it has the advantage of allowing for nonlinear enzyme kinetics, this approach yields essentially identical estimates of kinetic parameters as presented here.
(49) Hudak, N. S. Ph.D. Thesis, Columbia University, January 2007.
(50) Osina, M. A.; Bogdanovskaya, V. A.; Efremov, B. N. *Russ. J. Electrochem.* **2002**, *38*, 1082–1086.
(51) Osina, M. A.; Bogdanovskaya, V. A.; Tarasevich, M. R. *Russ. J. Electrochem.* **2003**, *39*, 407–412.
(52) Xu, F. *Appl. Biochem. Biotechnol.* **2001**, *95*, 125–133.
(53) Zille, A.; Munteanu, F. D.; Gubitz, G. M.; Cavaco-Paulo, A. *J. Mol. Catal. B: Enzym.* **2005**, *33*, 23–28.

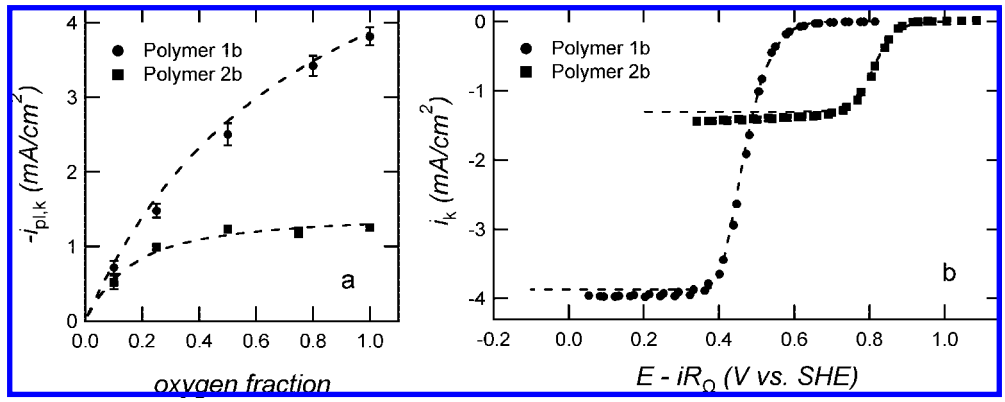

Figure 5. Comparison of analyzed experimental data to numerical prediction. (a) Internally limited plateau current, $i_{pl,k}$, for varying oxygen mole fraction. Each point is the result of a Koutecky−Levich analysis at the plateau current. Error bars indicate the standard deviation of three experiments. (b) Ohmic and Koutecky−Levich corrected polarization curves under 1 atm O_2. Dashed lines in both (a) and (b) indicate numerical model results simultaneously fit to both data sets.

Table 3. Kinetic Parameters of the Redox Polymer−Laccase Films

polymer	k_{cat} (s^{-1})	K_s (mM)	K_m (mM)	k_{cat}/K_s ($\times 10^{-5}$ s^{-1} M^{-1})	k_{cat}/K_m (s^{-1} M^{-1})
2a	86 ± 19	0.35 ± 0.09	350 ± 110	2.5 ± 0.85	(2.5 ± 1.0) × 10^2
2b	94 ± 33	0.54 ± 0.22	230 ± 130	1.8 ± 0.96	(4.0 ± 2.6) × 10^2
2c	310 ± 53	1.4 ± 0.26	110 ± 33	2.3 ± 0.58	(2.9 ± 1.0) × 10^3
2d	370 ± 31	2.0 ± 0.19	120 ± 15	1.9 ± 0.24	(3.0 ± 0.45) × 10^3
1a	430 ± 50	1.1 ± 0.20	4.4 ± 3.8	4.0 ± 0.91	(9.7 ± 8.6) × 10^4
1b	160 ± 7.9	0.81 ± 0.08	2.4 ± 1.6	2.0 ± 0.21	(6.9 ± 4.7) × 10^4
1c				2.0 ± 0.27	(9.1 ± 6.1) × 10^4
1d				0.90 ± 0.10	(1.2 ± 0.75) × 10^5

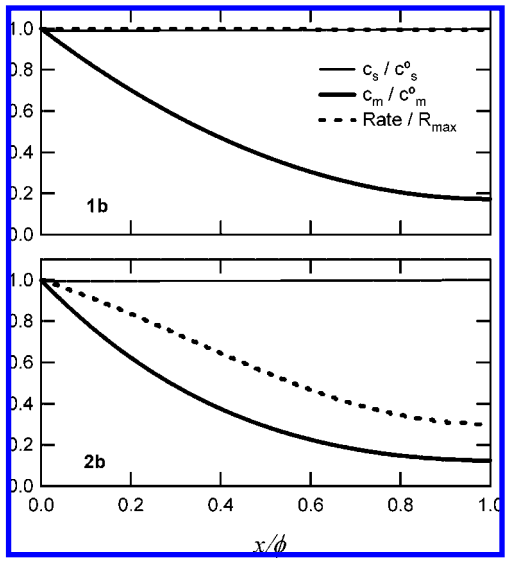

Figure 6. Simulated concentration and reaction rate profiles within the electrode film for polymers **1b** and **2b**. Conditions as in Figure 3, and operating at the Koutecky−Levich corrected plateau current, $i_{pl,k}$.

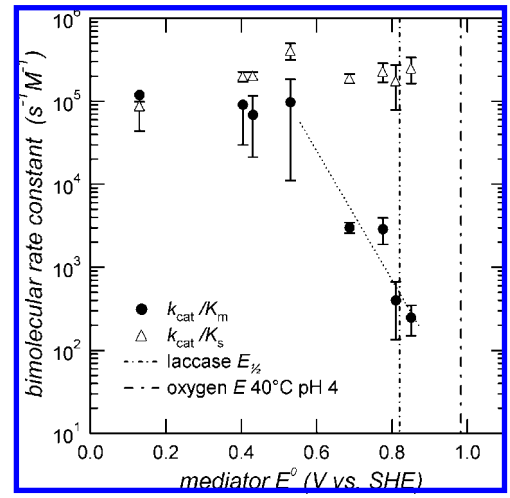

Figure 7. Effect of mediator redox potential, E^0_m, on laccase−mediator bimolecular rate constant, k_{cat}/K_m, and laccase−oxygen rate constant, k_{cat}/K_s. Also shown are redox potentials of laccase and O_2/H_2O at pH 4. A linear free energy region is observed for high E^0_m (small ΔE_{et}) and constant mediation rate at lower E^0_m values. Best-fit line in the linear free energy region is of the form given in eq 3.

Kinetic Sensitivity to Mediator Potential. Values of the Michaelis constant for the mediator, K_m, indicate the expected large kinetic variations brought about by varying mediator−enzyme overpotential, ΔE_{et}. From polymer **2a** to **1b**, K_m ranges from 2.4 to 350 mM. The dependence of the bimolecular rate constant for mediation, k_{cat}/K_m, on mediator redox potential is shown in Figure 7, which is similar to other figures of its type seen in the literature.[15,19,20,54,55] Two distinct regions are apparent. The first is a linear free energy region where rate increases exponentially with ΔE_{et}. The second is a plateau region where the rate constant becomes independent of ΔE_{et}, arriving at a constant value of approximately 9.4 × 10^4 s^{-1} M^{-1}. The transition to constant mediation kinetics occurs when ΔE_{et} reaches 250−300 mV, similar to diffusional mediator−enzyme systems operating in solution. Takagi et al. observe a plateau

(54) Coury, L. A.; Murray, R. W.; Johnson, J. L.; Rajagopalan, K. V. *J. Phys. Chem.* **1991**, *95*, 6034–6040.

(55) Barriere, F.; Ferry, Y.; Rochefort, D.; Leech, D. *Electrochem. Commun.* **2004**, *6*, 237–241.

at $\Delta E_{et} = 200$ mV in a system of various small molecules mediating diaphorase.[15] Zakeeruddin et al. report a mediation plateau reached at $\Delta E_{et} \approx 400$ mV for the mediation of glucose oxidase by osmium complexes similar to those attached to the supramolecular structure in the current work.[13] Based on these studies, significant differences in enzyme and mediator structure do not appear to significantly effect this optimal value of ΔE_{et}.

Application of eq 3 to the data of Figure 7 yields a specific bimolecular rate constant $(k_{cat}/K_m)^0$ of 490 s^{-1} M^{-1} and a transfer coefficient $\alpha = 0.48 \pm 0.07$, comparable to literature results for solution-phase systems and reflecting a reversible electron transfer mechanism.[15,19,20,54,55]

Discussion

The results described above show that redox polymer mediators with redox potentials approaching that of the enzyme exhibit a dramatic drop in catalytic performance, even when mediator concentration and charge transport rates are high. Values for the bimolecular rate constant in Figure 7 quantify this finding and agree with previous results in the literature for enzymes in solution phase. As seen from the individual fit parameters in Table 3, as ΔE_{et} approaches zero, the global rate constant k_{cat} generally decreases and K_m increases, signifying a decreased driving force for electron transfer from mediator to enzyme.

Polymers **2a** and **1a** follow a general trend of increasing k_{cat} with increasing ΔE_{et}. From eq 9, it can be seen that as electron transfer with the mediator becomes thermodynamically hindered by decreasing ΔE_{et} and k_{2m} becomes small, k_{cat} is expected to decrease, similar to previous findings in other enzyme systems.[56] Polymer **1b** appears to be an outlier, not fitting this trend. The relatively high value of k_{cat} even as ΔE_{et} becomes negative indicates a prominent role of k_{2s} in the rate. Experiments with lower-potential laccases in combination with these polymers has shown that, if ΔE_{et} becomes largely negative, current falls to zero.

The apparent Michaelis constant, K_s, for the laccase−oxygen reaction within the films was found to be on the order of 1 mM, varying linearly with k_{cat}, such that the bimolecular rate constant k_{cat}/K_s is relatively constant, with a mean value of 2.4×10^5 M^{-1} s^{-1}. For the same enzyme in solution, Xu finds Michaelis constants on the order of 40 μM, a factor of 25 less than the average values in the current study.[52] This disagreement may be due to our assumption of a unity partition coefficient or inhibition of oxygen−enzyme binding by osmium moieties, which are present at very high concentration compared to solution. The film electrode studies cited above[50,51,53] also report higher K_s in a film as compared to solution phase.

While the present model does not include oxygen partitioning, experiments were performed to detect partitioning by observing the steady-state reduction of oxygen at a platinum RDE covered by cross-linked osmium films.[57] The results, similar for all films, indicate the relationship $\kappa D_{s,f} = D_s/8$, where κ is the partition coefficient, D_s is the bulk solution diffusivity of oxygen, and $D_{s,f}$ is film diffusivity. Based on these observations, and estimating a diffusivity ratio $0.25 < D_{sf}/D_s < 0.4$,[58] we expect partition coefficients to fall in the range $0.3 < \kappa < 0.5$.

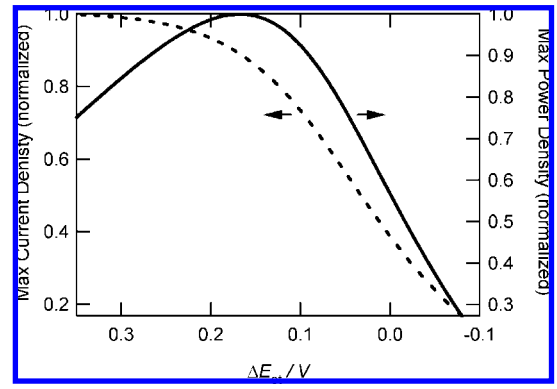

Figure 8. Predicted values for plateau current and maximum power for a planar laccase enzyme electrode operating in O_2-saturated solution with a nonlimiting anode poised at 0 V. Values are normalized to their maximum values: 1.6 mA/cm^2 and 0.8 mW/cm.^{2} All polymers are assumed to be identical, with the exception of kinetic parameters as determined by redox potential. Parameters used are typical of the biocatalytic films: $\phi = 1$ μm, $c_m = 200$ mM, $D_m = 1 \times 10^{-9}$ cm^2/s, $c_e = 5$ mM. Maximal power is obtained at $\Delta E_{et} = 0.17$ V.

Diffusivity ratios of $D_{sf}/D_s > 0.05$ are not expected to affect results significantly because the reacting film is not limited by oxygen mass transfer, as exemplified by the uniform substrate profiles in Figure 6.

We observed mean k_{cat}/K_s values of the same order but slightly lower than those reported by Xu for *T. versicolor* laccase in solution.[52] Xu does observe a dependence of k_{cat}/K_s on the reducing substrate, finding $k_{cat}/K_s = 4.4 \times 10^5$ M^{-1} s^{-1} for ABTS and $k_{cat}/K_s = 7.3 \times 10^5$ M^{-1} s^{-1} for methyl syringate.

Michaelis constants for mediation, K_m, were found to span a range from 2 to 350 mM, slightly higher but similar to findings by Brandi et al. for immobilized, mediated laccase from *T. villosa*.[59]

The observed k_{cat}/K_m plateau of 9.4×10^4 s^{-1} M^{-1} is lower than that seen in many solution-phase systems, although reported values vary widely across several orders of magnitude, depending on the system of interest. For example, the previously cited works of Zakeeruddin et al. and Takagi et al. report $k_{cat}/K_m \approx 10^6$ and 10^8 s^{-1} M^{-1} respectively.[13,15] Xu, studying the laccase system oxidizing a series of phenols, the natural substrate of laccase, found k_{cat}/K_m values as high as 5.5×10^6 s^{-1} M^{-1}, although the study did not extend to ΔE_{et} values high enough to observe a plateau.[20] Xu also observes $k_{cat}/K_m = 1.7 \times 10^5 s^{-1}$ M^{-1} at $\Delta E_{et} = 0$, 400 times the equivalent value in the current work. The comparatively low bimolecular rate constants reported here may indicate that kinetics are hindered in a dense, highly cross-linked film, where the T1 center of the laccase may be sterically blocked and both enzyme and mediator species have limited mobility. While the T1 copper is not reported to be as easily inhibited as the T2/T3 cluster, the presence of chloride in the films may impact the laccase negatively as well.[18,60]

Using the results reported above, the effect of mediator overpotential ΔE_{et} on the performance of a hypothetical biofuel cell device is shown in Figure 8, in which current density and power density are plotted as a function of ΔE_{et}. This plot was prepared using the Tafel relation in eq 3, assuming fixed values of other electrode parameters. Increasing ΔE_{et} results in increased current density, but a tradeoff is observed in the power

(56) Limoges, B.; Marchal, D.; Mavre, F.; Saveant, J. M. *J. Am. Chem. Soc.* **2006**, *128*, 2084–2092.
(57) Leddy, J. A.; Bard, A. J.; Maloy, J. T.; Saveant, J. M. *J. Electroanal. Chem.* **1985**, *187*, 205–227.
(58) van Stroe-Biezen, S. A. M.; Everaerts, F. M.; Janssen, L. J. J.; Tacken, R. A. *Anal. Chim. Acta* **1993**, *273*, 553–560.
(59) Brandi, P.; D'Annibale, A.; Galli, C.; Gentili, P.; Pontes, A. S. N. *J. Mol. Catal. B: Enzym.* **2006**, *41*, 61–69.
(60) Xu, F. *J. Biol. Chem.* **1997**, *272*, 924–928.

density curve, calculated assuming that the biocathode is coupled with a nonlimiting anode poised at 0 V. Maximum cell power is obtained for $E^0_m = 0.66$ V (SHE) for this system, corresponding roughly to polymer **2d**. This optimal value increases with increasing anode potential.

Conclusion

A series of osmium-based redox polymer mediators spanning a range of potentials was synthesized, and the performance of the resulting mediated laccase electrodes was found to be a function of mediator potential for $\Delta E_{et} \leq \sim 300$ mV. This relationship was revealed by detailed accounting of charge and species transport effects both within and external to the electrode. Bimolecular rate constants for laccase−oxygen reaction were found to be slightly lower in the catalytic film than in free solution, with an average value of 2.4×10^5 M^{-1} s^{-1}. The bimolecular rate constants for the mediator−laccase reaction were found to depend highly on mediator potential, as in solution-phase systems, although the magnitude was lower. For $\Delta E_{et} > 300$ mV, no dependence of ΔE_{et} on bimolecular rate constant was observed. When applied to biofuel cells, where maximal power density is the overall goal, these results inform the choice of optimal mediator potential.

Acknowledgment. The authors gratefully acknowledge financial support from the National Science Foundation (Award CTS-0239013) and the Air Force Office of Scientific Research (Award FA9550-06-1-0264).

Supporting Information Available: Lever analysis for prediction of the redox potentials shown in Table 1, swelling measurements of hydrated films, and cyclic voltammetry of redox polymer films. This material is available free of charge via the Internet at http://pubs.acs.org.

JA0781543